ORIGINAL RESEARCH

Frequent Dilatation of the Descending Aorta in Children With Hypoplastic Left Heart Syndrome Relates to Decreased Aortic Arch Elasticity

Inga Voges, MD*; Michael Jerosch-Herold, PHD*; Philip Wegner, MD; Christopher Hart, MD; Dominik Gabbert, PHD; Abdullah Al Bulushi, MD; Gunther Fischer, MD; Ana Cristina Andrade, MD; Hoang Minh Pham, MD; Ines Kristo, MD, PHD; Hans-Heiner Kramer, MD; Carsten Rickers, MD

***Background*—**Patients with hypoplastic left heart syndrome after a Norwood operation show dilatation and reduced distensibility of the reconstructed proximal aorta. Cardiac magnetic resonance imaging (CMR) and angiographic examinations indicate that the native descending aorta (DAo) is also dilated, but this has not been studied in detail.

***Methods and Results*—**Seventy-nine children with hypoplastic left heart syndrome in Fontan circulation (aged 6.3±3.2 years) and 18 control participants (aged 6.8±2.4 years) underwent 3.0-tesla CMR. Gradient-echo cine and phase-contrast imaging was applied to measure cross-sectional areas (CSAs), distensibility, pulse wave velocity, and the incremental elastic modulus of the thoracic aorta. CSA of the DAo in patients was also compared with published percentiles for aortic CSA. Patients had significantly larger CSA of the DAo at the level of pulmonary artery bifurcation (229.1±97.2 versus 175.7±24.3 mm/m^2, P=0.04) and the diaphragm (196.2±66.0 versus 142.6±16.7 mm/m^2, P<0.01). In 41 patients (52%), CSA of the DAo was >95th percentile level for control participants, and the incremental elastic modulus of the aortic arch and the DAo was higher than in patients with normal CSAs (arch: 90.1±64.3 versus 45.6±38.9 m/s; DAo: 86.3±53.7 versus 47.1±47.6 m/s; P<0.01). Incremental elastic modulus of the aortic arch and the DAo correlated with the CSA of the DAo (arch: r=0.5; DAo: r=0.49; P<0.01).

***Conclusions*—**Children with hypoplastic left heart syndrome frequently show dilatation of their DAo associated with increased stiffness of the aortic arch. Higher aortic impedance increases the afterload of the systemic circulation and likely contributes to the burden of the systemic right ventricle. **(*J Am Heart Assoc*. 2015;4:e002107 doi: 10.1161/JAHA.115.002107)**

Key Words: aortic elasticity • descending aortic dilatation • hypoplastic left heart syndrome • incremental elastic modulus • magnetic resonance imaging

The Norwood procedure has become routine therapy for patients with hypoplastic left heart syndrome (HLHS). Since its introduction in 1983, survival rates have risen, and the focus of clinical care has shifted to the prevention of long-term complications, which may result in a less favorable hemodynamic and functional status or even late mortality.

The fate of the reconstructed aorta in HLHS has been assessed in previous studies.[1–3] Cardis et al found increased stiffness and decreased distensibility in the reconstructed aortic arch by using echocardiography.[3] In a cardiac magnetic resonance imaging (CMR) study of a small cohort of HLHS patients (n=10), Biglino et al reported greater aortic pulse wave velocity (PWV) and reduced distensibility of the ascending aorta.[2] In addition, they found lower ascending aortic wave intensity and energy, suggesting abnormal ventricular–vascular coupling.[2] We previously demonstrated in 40 children with HLHS that the reconstructed aortic arch after Norwood procedure is significantly dilated and has reduced distensibility with negative effects on the function of the systemic right ventricle.[1] Further analyses of CMR studies and angiographic examinations at our institution suggested that not only do the reconstructed parts of the aorta show pathological changes but also the native descending aorta (DAo) is frequently dilated. DAo dilatation and increased DAo

From the Department of Congenital Heart Disease and Pediatric Cardiology, University Hospital of Schleswig-Holstein, Kiel, Germany (I.V., P.W., C.H., D.G., A.A.B., G.F., A.C.A., H.M.P., I.K., H.-H.K., C.R.); Department of Radiology, Brigham & Women's Hospital & Harvard Medical School, Boston, MA (M.J.-H.).

*Dr Voges and Dr Jerosch-Herold are co-first authors. Both first authors contributed equally to this work.

Correspondence to: Carsten Rickers, MD, Department of Congenital Heart Disease and Pediatric Cardiology, University Hospital of Schleswig-Holstein, Campus Kiel, Arnold-Heller-Str. 3, Kiel 24105, Germany. E-mail: rickers@pedcard.uni-kiel.de

Received April 21, 2015; accepted August 30, 2015.

stiffness may have an additional negative impact on right ventricular function and possibly increase the risk of mechanical aortic wall failure. Furthermore, it may result in higher susceptibility to early development of hypertension.

For the current study, we hypothesized that in patients with HLHS after a Norwood operation, the DAo is frequently dilated compared with healthy persons and that these changes may reflect an impaired elastic buffering capacity of the aortic arch. We systematically evaluated aortic dimensions, distensibility, PWV, and the incremental elastic modulus (E_{inc}), especially of the native DAo, in a large cohort of HLHS patients.

Methods

Patients

We investigated 79 children with HLHS who had undergone a Norwood operation between 1992 and 2008 as the first step of 3-stage surgical palliation. In 76 patients, 3-stage palliation with creation of an intra-atrial lateral tunnel at the third stage was completed. Three patients were examined after the second stage, which was the hemi-Fontan procedure. Interventions for recoarctation were necessary in 22 patients before or at the time of the hemi-Fontan procedure. Balloon angioplasty was performed in 20 of these patients, 1 patient underwent additional surgery after balloon angioplasty, and 2 patients were treated only surgically. None of the HLHS patients showed coarctation or recoarctation at the time of the CMR study.

Patients were compared with 18 age-matched heart-healthy control participants. Three control participants were referred for CMR due to suspected aortic arch abnormality because of recurrent airway infections, and 1 patient was supposed to have a coronary anomaly; all 4 children were found to have normal cardiovascular anatomy and cardiac function. The other control participants were recruited from hospital staff and from patients referred for diagnostic magnetic resonance imaging of the central nervous system. The latter underwent noncontrast CMR after magnetic resonance imaging of the central nervous system. For the CMR study, sedation with propofol and midazolam was used in all patients and some control participants. Control participants who underwent central nervous system magnetic resonance imaging received sedatives such as phenobarbital or chloral hydrate, and no further sedation was used for CMR. Heart rate, respiratory motion, oxygen saturation, and noninvasive blood pressure were monitored during examination. In 11 control subjects, CMR was performed without any sedation.

All parents or legal guardians gave their informed consent to the inclusion of their children in the study. The investigation protocol was approved by the local research ethics committee and was performed in accordance with the ethical standards laid down in the 1964 Declaration of Helsinki and its later amendments.

Cardiac Magnetic Resonance Imaging

CMR was performed in patients and controls using a 3.0-tesla scanner (Achieva 3.0T; Philips Medical Systems). A phased-array coil for cardiac imaging or, in small children, a coil for extremities (SENSE Cardiac coil, SENSE Flex-L coil; Philips Medical Systems) was placed on the chest.

Gradient-echo cine imaging with retrospective ECG gating was performed for sagittal and coronal–oblique as well as axial slices to cover the entire thoracic aorta and to assess aortic CSAs (Figure 1). The sequence parameters were as follows: field of view 280×224 mm, voxel size 1.88×1.94×5 mm (slice thickness), repetition time/echo time 4.4/2.5 ms, 25 cardiac phases, no slice gap, non–breath hold, 2 repetitions, ≈20 to 30 seconds for acquisition time, segmentation factor 10 lines/k-space segment, temporal resolution ≈60 ms per phase, and 3 to 5 minutes for all cine acquisitions.

Phase-contrast cine imaging was used for evaluation of aortic PWV (1) between the ascending aorta at the level of the sinutubular junction and the proximal DAo at the level of the pulmonary artery bifurcation (PWV_1) and (2) between the proximal DAo at the level of the pulmonary artery bifurcation

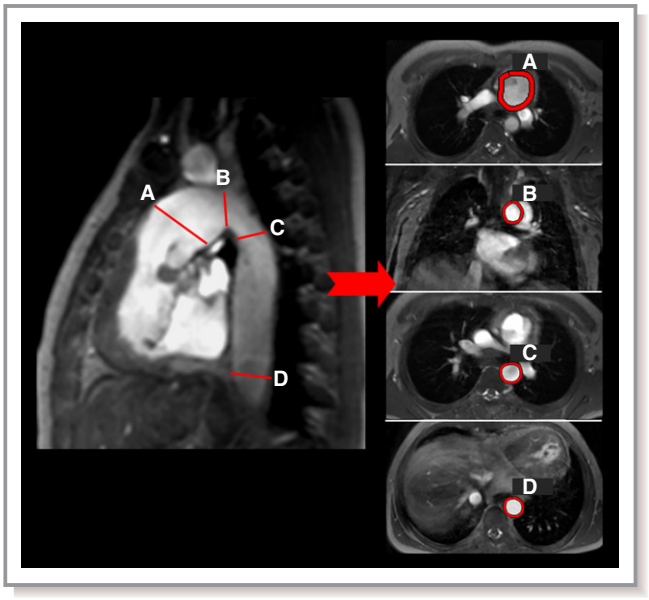

Figure 1. Sagittal, axial, and coronal images demonstrate the assessment of aortic cross-sectional areas. The measuring points shown are (A) ascending aorta, (B) aortic arch, (C) DAo at the level of the pulmonary artery bifurcation, and (D) DAo at the level of the diaphragm. DAo indicates descending aorta.

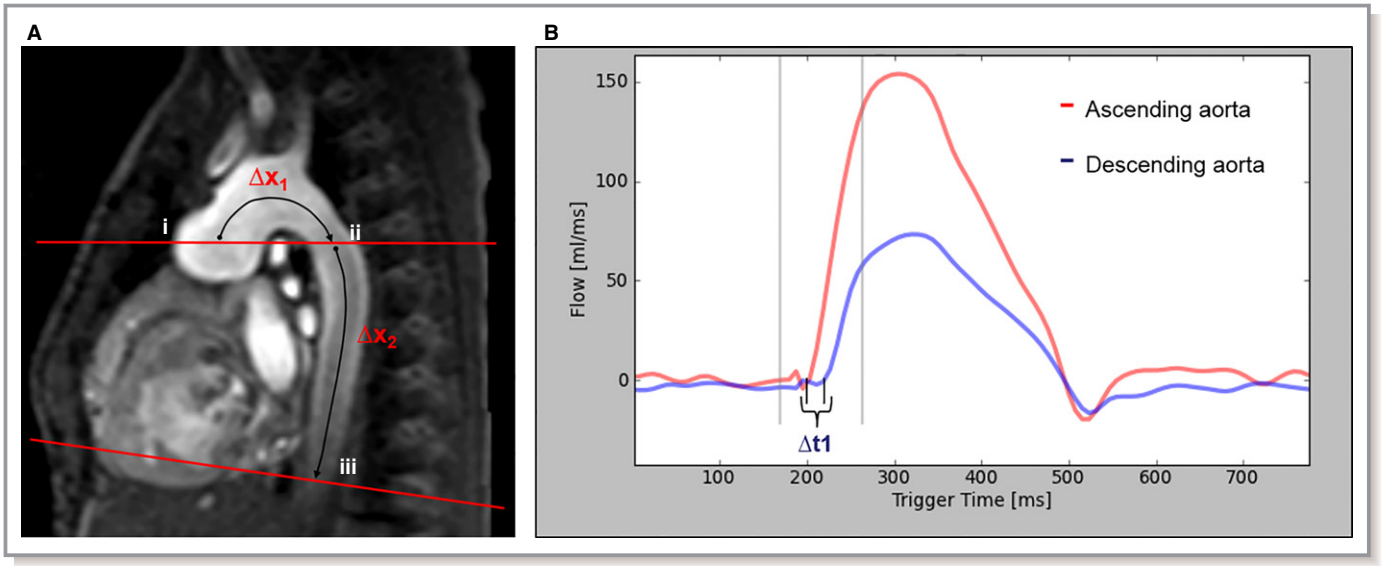

Figure 2. A, This sagittal–oblique cardiac magnetic resonance image shows the slice positioning for aortic phase-contrast flow measurements in the ascending aorta and DAo. Aortic flow was assessed at 3 sites: (i) ascending aorta, (ii) proximal DAo at the pulmonary artery bifurcation, and (iii) DAo at the diaphragm. For PWV assessment, the distance was measured between the ascending aorta and the proximal DAo at the level of the pulmonary artery bifurcation (Δx1) and between the proximal DAo and the DAo at the level of the diaphragm (Δx2). B, This image shows the flow curves in the ascending and proximal DAo at the level of the pulmonary artery bifurcation. The time delay (Δt) between both curves was measured using the cross-correlation method.[4] PWV was calculated according to this formula: Δx/Δt. DAo indicates descending aorta; PWV, pulse wave velocity.

and the DAo at the level of the diaphragm (PWV_2). Phase-contrast images were acquired for 2 slice planes: 1 slice intersected the aorta at the sinutubular junction and the DAo at the level of the pulmonary artery bifurcation at an approximately right angle, and another slice was positioned perpendicular to the aorta above the diaphragm (Figure 2). The acquisition of phase-contrast imaging data was performed with the patient breathing freely, and the following scan parameters were used: field of view 270×270 mm, voxel size 1.64×1.4×7 mm, repetition time/echo time 4.4/2.7 ms, velocity encoding strength 200 cm/s, 1 repetitions, 45 to 75 seconds for acquisition time, 80 phases, 1 k-space segmentation factor. The maximal temporal resolution corresponded to 2× repetition time, equaling ≈9 ms. In patients with strong breathing excursions, the number of repetitions was 2. Phase-contrast imaging for assessment of PWV_1 could not be performed in 20 patients, and PWV_2 could not be assessed in 36 patients. The causes of failure of phase-contrast imaging were (1) susceptibility artifacts from implanted devices or from coils previously implanted to close collaterals and (2) early awakening from sedation. Artifacts related to coils or devices lead to signal loss in phase-contrast imaging, field inhomogeneities, and errors in blood flow velocity measurements.

Image quality was judged by 2 independent observers using a 5-point scale: 5, very good/no artifacts; 4, good/only a few artifacts; 3, fair/artifacts did not influence image quality; 2, poor/artifacts influence image quality; and 1, very poor/not assessable because of artifacts. Images with grades 1 and 2 were not used for further assessments.

Data Analysis

All CMR images were analyzed with dedicated software (Extended MR WorkSpace, version 2.6.3.2 HF3 2010; Philips Medical Systems).

Aortic CSAs were measured from coronal–oblique and axial cine images. The measuring locations were (1) ascending aorta, (2) aortic arch, (3) DAo at the level of the pulmonary artery bifurcation, and (4) DAo at the level of the diaphragm (Figure 1). All measurements of aortic dimensions were done for the phase showing maximal distension of the aorta. CSAs were indexed by body surface area. In a subanalysis, we compared aortic CSA of the DAo at the level of the diaphragm with normal values collected by our group.[4]

Aortic distensibility was determined at the same 4 locations used for aortic area measurements. For aortic distensibility, areas were measured at the times of maximal and minimal distension. Distensibility was defined by the following equation[5]:

$$\text{Distensibility (expressed in } 10^{-3}\text{mm Hg}^{-1}) = (A_{max} - A_{min})/[A_{min} \times (P_{max} - P_{min})]$$

In this equation, A_{max} and A_{min} represent the maximal and minimal aortic CSAs, and P_{max} and P_{min} are the systolic and

diastolic blood pressures, respectively. Noninvasive blood pressures were obtained during CMR using a magnetic resonance imaging–compatible monitor with sphygmomanometer (Invivo Precess 3160; Invivo) with the cuff placed around the right arm.

Aortic PWV was calculated using the following equation:

$$\mathrm{PWV(expressed\ in\ m/s)} = \Delta x/\Delta t$$

,In this equation, Δx is the aortic segment length, and Δt is the time delay of the systolic upstroke in the distal flow curve relative to the proximal flow curve (Figure 2). The time delay was determined by maximizing the cross-correlation between the systolic upstroke portions of the proximal and distal flow waveforms; this method has been validated for estimating delay time.[6]

Although PWV is generally used as a marker of the elastic properties of the vessel wall, changes in PWV can also occur as a result of alterations in vessel geometry. To separate vessel dilation from changes in the elastic properties, we used the Moens–Korteweg equation to calculate the E_{inc} from the measured PWV, the wall thickness (represented as h), and the inner radius (represented as r_i) of the vessel[7]:

$$\mathrm{PWV} = [(E_{inc} \times h)/(2\rho \times r_i)]^{1/2}.$$

For the density of blood (represented as ρ), a default value of 1 g/mL was used.

To measure the aortic wall thickness, endo- and epivascular borders at 2 aortic positions (ie, the aortic arch and the DAo at the diaphragm) were drawn by using coronal–oblique and axial cine sequences. Aortic wall area was then calculated by subtracting the inner aortic area from the outer aortic area. Furthermore, the radius of the inner (represented as r_i) and the outer aortic area (represented as r_o) was measured. Average aortic wall thickness was finally calculated using the following equation:

$$\mathrm{Aortic\ wall\ area}/(\mathrm{pi} \times (r_i + r_o)).$$

Aortic CSA, PWV, and aortic wall thickness were measured twice by 2 independent observers. In addition, others have reported excellent interobserver agreement and reproducibility for systolic and diastolic aortic area measurements and for calculation of PWV.[8]

Statistical Analysis

Statistical analysis was performed with MedCalc (version 12.0.4.0; MedCalc Software) and the R program (R version 3.1.2; R Foundation for Statistical Computing). Data are presented as mean±SD. Interrater agreement was measured by the intraclass correlation coefficients for all aortic CSAs, PWVs, and aortic wall thicknesses. The method of Bland and Altman was used to evaluate the difference between 2 measurements. The 5th and 95th percentile limits of agreement for the mean difference were defined by assuming, based on the central limit theorem, a normal distribution for the mean difference and calculating the limits as ±1.96 times the SD of the difference. The 5th and 95th limits of agreement for the differences between 2 measurements were estimated from its empirical distribution. The Mann–Whitney *U* test for independent samples was used to compare patients and control participants. Correlations were assessed by Pearson's moment product correlation. A 1-way comparison of continuous variables between groups was performed with the Kruskal–Wallis test. Dunn's test was applied for pairwise comparison between groups following the Kruskal–Wallis test. *P* values for post hoc pairwise comparison were adjusted with Bonferroni's method. All comparison tests were 2-tailed, and *P* values <0.05 were considered statistically significant.

Results

HLHS patients and control participants were comparable in age, body height, body weight, body surface area, and pulse pressure. Oxygen saturation, heart rate, and mean arterial pressure were lower in the patient group (Table 1).

Aortic Dimensions

Data on aortic dimensions are presented in Table 2. Patients with HLHS showed significantly increased CSA indexed by body surface area of the DAo at the level of the pulmonary artery bifurcation and at the diaphragm. Indexing by body surface area significantly reduced the variance of aortic dimensions in healthy control participants. Indexing our

Table 1. Characteristics of the Study Population

Parameter	HLHS (n=79)	Control (n=18)	*P* Value
Age, y	6.3±3.2	6.8±2.4	0.18
Female/male, n	25/57	7/11	
Body weight, kg	21.4±10.4	23.6±8.0	0.08
Body height, cm	113.7±20.2	118.9±17.3	0.19
BSA, m^2	0.8±0.3	0.9±0.2	0.11
Heart rate, bpm	80.4±16.0	91.1±14.3	0.02
MAP, mm Hg	58.8±10.2	71.1±12.7	<0.01
Pulse pressure, mm Hg	41.8±8.9	41.5±8.8	0.99
Oxygen saturation, %	89.8±4.3	96.1±2.6	<0.01

Data are expressed as mean±SD. *P* values are from the from the Mann–Whitney *U* test. BSA indicates body surface area; HLHS, hypoplastic left heart syndrome; MAP, mean arterial pressure.

Table 2. Comparison of Aortic Dimensions, Distensibility, PWV, and E_{inc} in Patients and Heart-Healthy Control Participants

Parameter	HLHS (n=79)	Control (n=18)	*P* Value
Cross-sectional areas, mm^2			
Ascending aorta	686.0±255.3	303.6±98.9	<0.001
Aortic arch	332.3±158.3	230.1±110.4	<0.01
Descending aorta, PA bifurcation	184.8±102.6	154.7±47.2	0.49
Descending aorta, diaphragm	159.3±78.0	125.5±33.4	0.11
Cross-sectional area, mm/m^2			
Ascending aorta	861.2±200.4	341.0±78.2	<0.001
Aortic arch	429.2±148.8	224.9±67.8	<0.001
Descending aorta, PA bifurcation	229.1±97.2	175.7±24.3	0.04
Descending aorta, diaphragm	196.2±66.0	142.6±16.7	<0.001
Distensibility, 10^{-3} mm Hg^{-1}			
Ascending aorta	4.1±1.8	11.3±4.3	<0.001
Aortic arch	4.7±2.6	10.0±2.6	<0.001
Descending aorta, PA bifurcation	10.6±4.8	9.4±2.8	0.34
Descending aorta, diaphragm	12.4±6.5	9.9±3.2	0.21
PWV, m/s*			
PWV_1	3.7±1.4	3.2±0.4	0.51
PWV_2	3.7±1.3	4.0±1.0	0.24
E_{inc}			
Aortic arch	69.8±57.5	46.0±14.8	0.63
Descending aorta	67.2±54.0	67.1±32.6	0.43

Data are expressed as mean±SD. *P* values are from the from the Mann–Whitney *U* test. E_{inc} indicates incremental elastic modulus; HLHS, hypoplastic left heart syndrome; PA, pulmonary artery; PWV, pulse wave velocity; PWV_1, pulse wave velocity in a segment that included the ascending aorta at the level of the sinotubular junction and the proximal descending aorta at the level of the PA bifurcation; PWV_2, pulse wave velocity in a segment between the proximal descending aorta at the level of the PA bifurcation and the descending aorta at the level of the diaphragm.

*Phase-contrast imaging for assessment of aortic arch E_{inc} and PWV_1 could not be performed in 20 patients and descending aorta E_{inc} and PWV_2 could not be assessed in 36 patients.

measurements by height would not materially change the results.

Overall, 41 HLHS patients (52%) had a CSA of the DAo at the level of the diaphragm above the normal range (ie, >95th percentile of healthy persons)[4] (Figure 3). Figure 4 shows the proportions of patients with an aortic CSA >95th percentile for all aortic locations, illustrating that dilation of the DAo was frequent, with similar proportions for male and female participants. Characteristics of HLHS patients with DAo CSAs >95th and ≤95th percentiles for healthy children are listed in Table 3. The size of the ascending aorta and the aortic arch were not significantly different between the subgroups (Table 4).

PWV and E_{inc}

The PWV in the aortic arch and the thoracic DAo was significantly higher in HLHS patients with CSA of the DAo above the normal range compared with HLHS patients with a CSA of the DAo within the normal range (Table 4).

In the entire patient cohort, aortic arch PWV correlated significantly with the CSA of the DAo at the level of the diaphragm (Spearman's ρ=0.46; $P<1^{-4}$) and at the level of the pulmonary artery bifurcation (Spearman's ρ=0.5; $P<1^{-5}$). The PWV in the aortic arch of HLHS patients with dilated DAo trended higher compared with control participants (*P*=0.08), but there was no significant difference for PWV in the DAo.

Patients with CSA of the DAo >95th percentile had a higher E_{inc} in the aortic arch compared with patients with a CSA of the DAo ≤95th percentile (Figure 5). E_{inc} in the DAo was higher compared with patients with a CSA of the DAo ≤95th percentile (Table 4, Figure 5). Patients with a normal CSA of the DAo showed a trend toward a lower E_{inc} of the DAo compared with control participants (47.1±47.6 versus 63±33.3, adjusted *P*=0.071).

E_{inc} of the aortic arch and the DAo correlated significantly with the CSA of the DAo at the level of the diaphragm (aortic arch E_{inc}: *r*=0.5, *P*=0.0001; DAo E_{inc}: *r*= 0.49, *P*=0.001) (Figure 6) and at the level of the pulmonary artery bifurcation

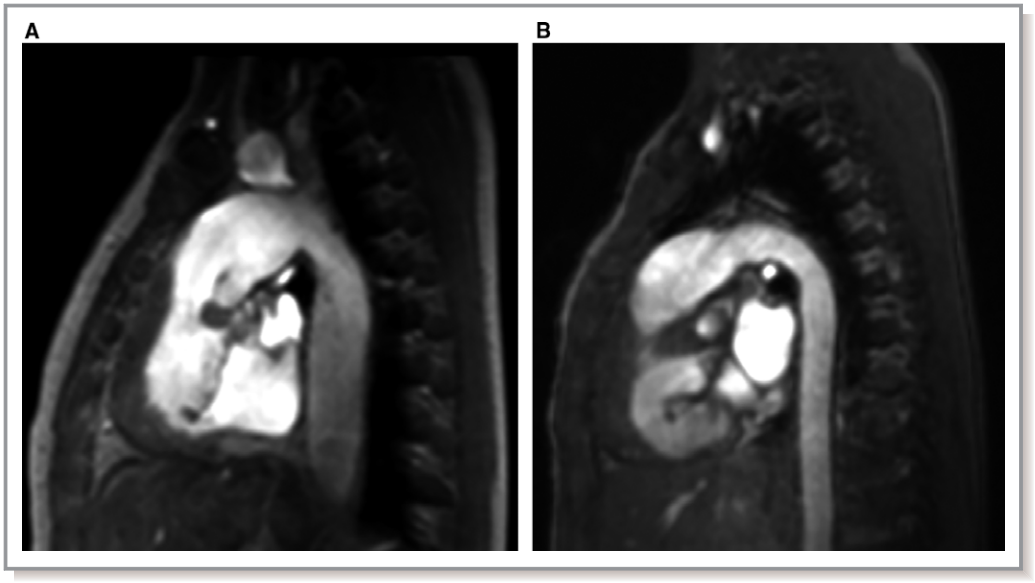

Figure 3. Sagittal multiplanar reconstruction images of the thoracic aorta in 2 patients with hypoplastic left heart syndrome. Left-sided image (A) shows a boy aged 3 years with dilatation of the entire thoracic aorta. Right-sided image (B) shows a boy aged 12 years with a normal-sized thoracic aorta.

(aortic arch E_{inc}: r=0.62, P<0.0001; DAo E_{inc}: r=0.47, P=0.002). These correlations remained significant when aortic CSA was not indexed by body surface area. HLHS patients were also subdivided into 2 subgroups depending on whether the E_{inc} in the aortic arch was >95th percentile for E_{inc} in healthy controls. Dilation of the DAo was significantly more frequent in the subgroup with abnormally high E_{inc} in the aortic arch (Figure 7).

The impedance of the DAo, defined as PWV divided by maximum CSA,[9] was significantly lower in HLHS patients with dilated DAo compared with those without dilation (153±56.5 Pa s cm^{-3} versus 218±97.6 Pa s cm^{-3}, P<0.01).

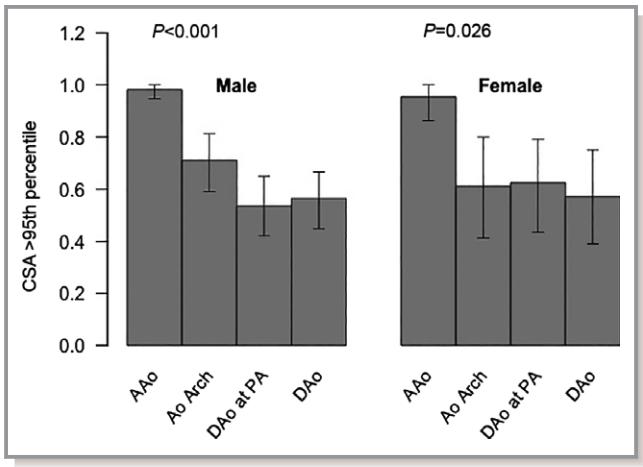

Figure 4. Proportions of patients with an aortic CSA >95th percentile for all aortic locations and separately plotted for male and female participants. AAo, ascending aorta; Ao indicates aorta; CSA, cross-sectional area; DAo, descending aorta; PA, pulmonary artery.

Aortic Distensibility

Distensibility of the DAo was not significantly different between patient and control groups, but the distensibility of the DAo at the diaphragm level showed a trend toward

Table 3. Comparison of Patients With an Aortic CSA >95th Percentile Versus Patients With an Aortic CSA ≤95th Percentile

Parameter	HLHS, Descending Aortic CSA ≤95th Percentile (n=38)	HLHS, Descending Aortic CSA >95th Percentile (n=41)	*P* Value
Age, y	6.6±3.6	6.0±2.8	0.59
Female/male, n	12/26	10/31	
Body weight, kg	21.3±11.7	21.5±9.1	0.73
Body height, cm	113.7±22.1	113.6±18.6	0.56
BSA, m^2	0.8±0.3	0.8±0.2	0.92
Heart rate, bpm	82.0±15.6	78.9±16.4	0.32
Pulse pressure, mm Hg	43.6±9.0	40.0±8.5	0.03
MAP, mm Hg	57.8±10.8	59.8±9.5	0.29
Oxygen saturation, %	90.2±4.4	89.3±4.4	0.33

Data are expressed as mean±SD. *P* values are from the from the Mann–Whitney *U* test. bpm indicates beats per minute; BSA , body surface area; CSA, cross-sectional areas; HLHS, hypoplastic left heart syndrome; MAP, mean arterial pressure.

Table 4. Comparison of Aortic Dimensions, Distensibility, PWV, and E_{inc} in Patients With an Aortic CSA >95th Percentile Versus Patients With an Aortic CSA ≤95th Percentile

Parameter	HLHS, Descending Aortic CSA ≤95th Percentile (n=38)	HLHS, Descending Aortic CSA >95th Percentile (n=41)	*P* Value
CSA, mm^2			
Ascending aorta	685.8±272.6	686.1±241.3	0.83
Aortic arch	301.4±128.2	360.5±178.7	0.10
Descending aorta, PA bifurcation	142.7±63.4	222.8±116.4	<0.01
Descending aorta, diaphragm	119.5±44.4	196.1±84.6	<0.01
CSA, mm^2/m^2			
Ascending aorta	863.4±176.7	859.1±222.9	0.95
Aortic arch	407.6±151.8	449.0±145.4	0.22
Descending aorta, PA bifurcation	182.6±62.7	271.0±104.1	<0.01
Descending aorta, diaphragm	151.2±38.8	237.9±58.1	<0.01
Distensibility, 10^{-3} mm Hg^{-1}			
Ascending aorta	4.0±1.8	4.1±1.9	0.51
Aortic arch	4.4±2.6	4.9±2.6	0.41
Descending aorta, PA bifurcation	11.3±5.8	10.0±3.6	0.50
Descending aorta, diaphragm	13.5±6.5	11.3±6.5	0.07
PWV, m/s			
Aortic arch (PWV_1)	3.2±1.1	4.2±1.6	<0.01
Descending aorta (PWV_2)	3.4±1.3	4.0±1.1	0.04
E_{inc}			
Aortic arch	45.6±38.9	90.1±63.3	<0.01
Descending aorta	47.1±47.6	86.3±53.7	<0.01

Data are expressed as mean±SD. *P* values are from the from the Mann–Whitney *U* test. CSA indicates cross-sectional areas; E_{inc}, incremental elastic modulus; HLHS, hypoplastic left heart syndrome; PA, pulmonary artery; PWV, pulse wave velocity; PWV_1, pulse wave velocity in a segment that included the ascending aorta at the level of the sinotubular junction and the proximal descending aorta at the level of the PA bifurcation; PWV_2, pulse wave velocity in a segment between the proximal descending aorta at the level of the PA bifurcation and the descending aorta at the level of the diaphragm.

reduced values in HLHS patients with a CSA >95th percentile of the DAo for control participants (Table 4). Ascending aortic and aortic arch distensibility were significantly reduced in patients compared with control participants (Table 2).

Reproducibility of Aortic Measurements

Measurements of aortic CSA and PWV proved to be highly reproducible. The intraclass correlation coefficients and mean interobserver differences for the aortic CSA, PWV, and aortic wall thickness measurements are shown in Table 5.

Discussion

This study demonstrates that in HLHS patients after Fontan palliation, aortic dilatation is not limited to the reconstructed parts of the aorta but extends to the native DAo. Nearly half of HLHS patients showed CSA values >95th percentile of CSA in the DAo in healthy controls. In the subgroup of HLHS patients with dilated CSA, we discovered functional correlates such as increased E_{inc} of the aortic arch and the DAo. E_{inc} in HLHS patients correlated strongly with CSA of the DAo. Although the structural and functional changes of the reconstructed aortic arch are a consequence of surgical intervention, our findings for the native DAo may reflect secondary changes due to abnormal blood flow, higher E_{inc} in the reconstructed aortic arch, or possibly primary structural abnormalities of the aortic wall in the DAo.

Aortic Dimensions

Dilatation of the DAo may be due to abnormal aortic blood flow patterns such as vortex formation, which is known to increase wall shear stress.[10–12] Because the dilatation involves the whole length of the DAo, it is distinct from a circumscribed poststenotic dilation, which is explained by the fast and turbulent flow behind a narrowing.[13,14] We did not

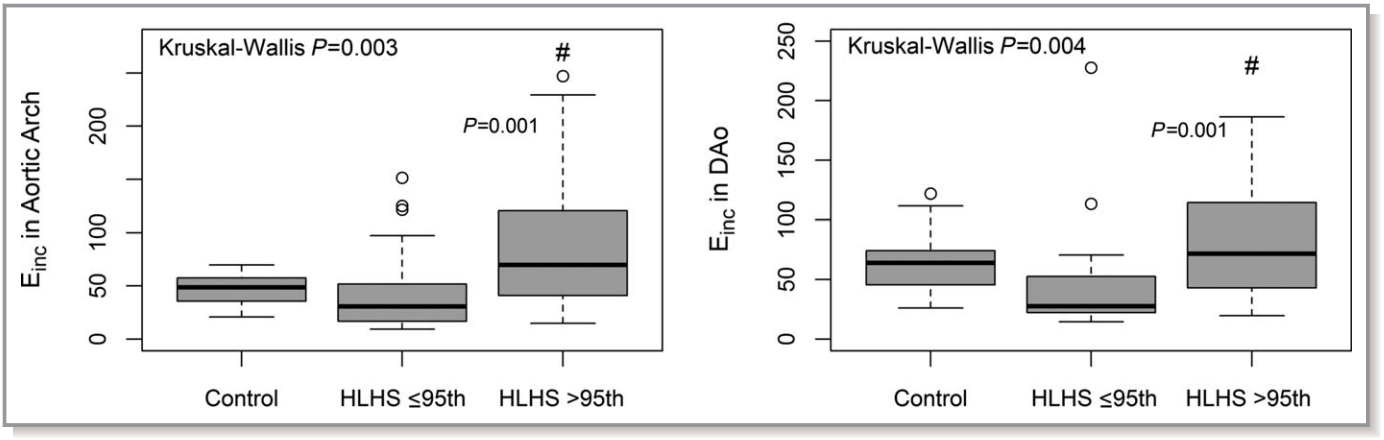

Figure 5. Box-and-whisker plot showing E_{inc} in the aortic arch (left graph) and E_{inc} in the DAo (right graph) in control participants, in HLHS patients with descending aorta size ≤95th percentile, and in HLHS patients with descending aorta size >95th percentile. #HLHS >95th versus ≤95th percentile, adjusted *P*=0.001. A circle represents a single data point. DAo indicates descending aorta; E_{inc}, incremental elastic modulus; HLHS, hypoplastic left heart syndrome.

observe any association between the presence of previous aortic coarctation and DAo dilatation. Vascular abnormalities were documented in a histological study by Niwa et al in various types of congenital heart disease,[15] but unfortunately, the cohort did not include HLHS samples. They found fragmentation of elastic fibers, increase in collagen content, and loss of smooth muscle cells, which are likely to predispose to aortic dilatation.

Aortic PWV, incremental elastic modulus, and distensibility

HLHS patients with CSA of the DAo above the normal range had significantly increased PWV and E_{inc} in the thoracic aorta and showed a trend toward reduced distensibility of the DAo at the diaphragm level compared with patients with CSA of the DAo within the normal range. These findings suggest that the native DAo has increased stiffness. Distensibility and PWV are well-accepted markers of arterial stiffness.[16] The E_{inc} was derived as an additional measure in this study to avoid

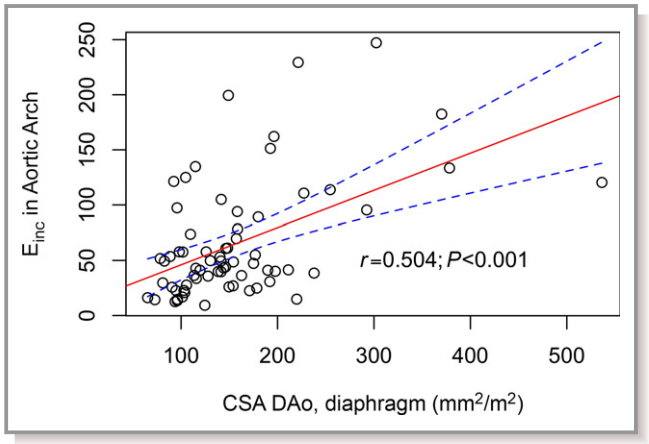

Figure 6. In HLHS, E_{inc} in the arch correlated positively with the averaged CSA in the DAo. This suggests that changes in elastic wall properties are associated with DAo dilation (r=0.5 is for Pearson's product-moment correlation). A circle in this graph represents a single data point. CSA indicates cross-sectional areas; DAo, descending aorta; E_{inc}, incremental elastic modulus; HLHS, hypoplastic left heart syndrome.

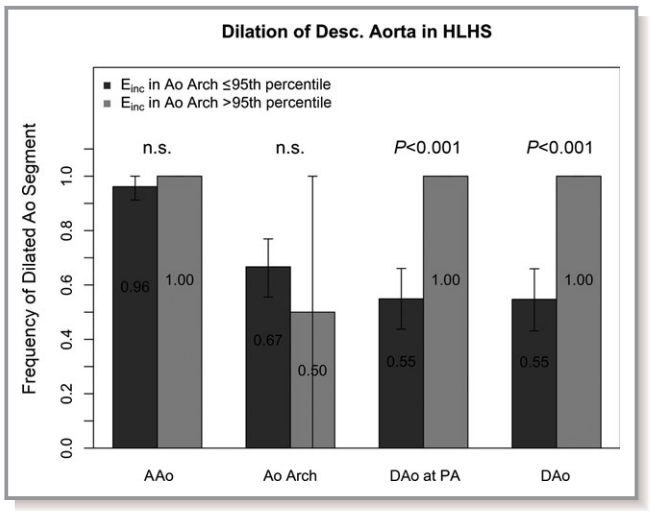

Figure 7. Frequency of dilated aortic segments in HLHS patients with an E_{inc} in the aortic arch ≤95th percentile and in HLHS patients with an E_{inc} in the aortic arch >95th percentile. Error bars represent the 95% confidence limits for the observed frequency of dilation of an aortic segment, obtained by the bootstrapping method. Dilation in the aortic segments downstream from the aortic arch was significantly more frequent in the group with abnormally high E_{inc} in the aortic arch. The *P* values for comparison of proportions in the groups with and without E_{inc} in the aortic arch >95th percentile were adjusted by the Bonferroni method. AAo indicates ascending aorta; Ao, aorta; DAo, descending aorta; E_{inc}, incremental elastic modulus; HLHS, hypoplastic left heart syndrome; n.s., not significant; PA, pulmonary artery.

Table 5. Reproducibility of Aortic Measurements

Parameter	Interobserver Differences (5th/95th Limits of Agreement)	ICC
Cross-sectional areas, mm^2		
Ascending aorta	17.92 (−27.72/63.55)	0.994
Aortic arch	−0.33 (−24.68/24.02)	0.998
Descending aorta, PA bifurcation	9.06 (−18.92/37.04)	0.98
Descending aorta, diaphragm	2.50 (−10.28/15.27)	0.997
PWV, m/s		
PWV_1	−0.09 (−0.39/0.57)	0.998
PWV_2	−0.11 (−0.96/0.74)	0.947
Wall thickness, mm		
Aortic arch	0.013 (−0.01/0.04)	0.991
Descending aorta	0.002 (−0.03/0.02)	0.992

ICC indicates intraclass correlation coefficient; PA, pulmonary artery; PWV, pulse wave velocity; PWV_1, pulse wave velocity in a segment that included the ascending aorta at the level of the sinotubular junction and the proximal descending aorta at the level of the PA bifurcation; PWV_2, pulse wave velocity in a segment between the proximal descending aorta at the level of the PA bifurcation and the descending aorta at the level of the diaphragm.

confounding by differences in vessel diameter.[17,18] Reduced aortic distensibility of the reconstructed aortic arch using graft material was reported by Cardis et al and by our group.[1,3]

Mathematically, the PWV can be predicted according to the Moens–Korteweg equation: $PWV=[(E_{inc}\times h)/(2\rho\times r_i)]^{1/2}$. In this equation, E_{inc} can be estimated from the first derivative of the stress–strain relationship, h is the wall thickness, ρ indicates the blood density, and r_i is the vessel inner radius.[7] Vessel wall thickness has to increase to cause an increase of PWV, whereas the inner radius of the vessel would have to decrease to achieve an increase of PWV. The PWV has been widely used in previous studies to assess changes in the elastic properties of vessel walls.[16,19] An implicit assumption has to be that factors extraneous to the elastic properties of a vessel wall but that have a direct effect on the PWV do not become confounding factors. The dilation of the aorta in HLHS patients can be such a confounding factor. In the present study of HLHS patients and healthy control participants, with large differences in aortic dimensions between groups, it became expedient to isolate changes in the elastic properties in the vessel wall from changes in vessel dimensions.

We calculated E_{inc} from the PWV and wall thickness and found that increased E_{inc} in the aortic arch and the DAo was strongly associated with an enlarged DAo (>2 SD) (Figure 6). At least 2 conceivable mechanisms could account for dilation and increased E_{inc}. First, the extreme size of the neoaortic root and the surgically reconstructed aortic arch (Figure 1) are likely to cause abnormal blood flow patterns (eg, enhanced helical flow or vortex formation) that affect the thoracic aorta by increasing wall stress, which can cause vessel wall dilatation. Other studies investigating aortic blood flow patterns (eg, increased vertical flow) in patients with bicuspid aortic valves or aortic aneurysms support this assumption[11,20]; however, the consequences of the disharmonious shape of the aortic arch and blood flow patterns have not yet been studied by recently introduced CMR techniques (eg, 4-dimensional phase-contrast magnetic resonance imaging). The second interpretation considers the impact of an intrinsically increased stiffness of the aortic arch on CSA in a downstream segment of the DAo, independent of abnormal flow patterns. Intrinsic structural aortic wall abnormalities, already observed in several forms of congenital heart disease, may also lead to higher arterial stiffness and PWV in HLHS.[15,21] A stiffer aortic arch would result in reduced elastic buffering capacity, meaning that the DAo may have to cope with more wall stress and energy dissipation than if the aortic arch had normal elastic properties. This interpretation is supported by the strong association between E_{inc} in the aortic arch and CSA of the DAo (Figure 6). HLHS patients with increased stiffness of the aortic arch, assessed by E_{inc}, are at a significantly higher risk of dilation of the DAo compared with HLHS patients with normal E_{inc} in the aortic arch (Figure 5).

We found a trend toward lower E_{inc} of the DAo in patients with CSA of the DAo in the normal range compared with control participants. This finding was unexpected and may reflect differences in aortic wall loading conditions between HLHS patients and control participants because the latter had a significantly higher mean arterial pressure. It is known that an increase of the pressure load on the arterial wall shifts the load-bearing balance from elastin fibers to the stiffer collagen fibers.[18] It is plausible that the E_{inc} trends higher in the control group compared with HLHS patients with DAo dimensions within the normal range. In fact, differences in loading conditions have rendered it difficult in other diseases such as hypertension to distinguish between intrinsic changes in the aortic wall and an increase in aortic stiffness due to higher loading in hypertension. The same concern is of much less relevance in the comparison between our 2 HLHS subgroups because neither has a significant difference in mean arterial pressure. Furthermore, the differences in E_{inc} between the 2 HLHS subgroups could be ascertained in this study with a much higher level of statistical significance than any differences between HLHS patients and control participants.

Although aortic E_{inc}, PWV, and distensibility provide similar information about aortic function,[16] we found significantly increased E_{inc} ($P<0.01$) and PWV ($P=0.04$) but only a trend for a decrease of aortic distensibility at the level of the diaphragm ($P=0.07$) in patients with a dilated DAo compared with those with DAo dimensions within the normal range. This is no contradiction because methodological differences between

either E_{inc} and PWV and distensibility assessment have to be taken into account. Aortic distensibility measurements depend on an estimate of pulse pressure, but the change of pulse pressure along the aorta is itself affected by size.[22] Indeed, if we calculate the impedance of the DAo (defined as PWV divided by maximum CSA),[9] we find significantly lower vascular impedance for HLHS patients with dilated DAo (ie, >95th percentile for CSA in normal controls) compared with those without dilatation ($P<0.001$). For constant cardiac output, impedance determines pulse pressure and the drop of mean pressure in a vessel. If pulse pressure along the DAo of HLHS patients depends on the impedance of the DAo, then this can potentially affect estimates of distensibility in which peripheral pulse pressure is used as a surrogate for central aortic pulse pressure. E_{inc} and PWV do not depend on estimates of central pulse pressure and thus may be more reliable.

A consequence of aortic stiffening is the increase of ventricular afterload and myocardial oxygen consumption.[19] These consequences are of particular concern in patients with HLHS because it has been shown that the systemic right ventricle is maladapted to function as a systemic pressure pump and thus is more sensitive to increased afterload than the left ventricle.[1,23] Furthermore, the alterations of the vascular elastic properties may result in a higher susceptibility for early development of hypertension. PWV has been shown to be a predictor of future changes in systolic blood pressure and future development of hypertension.[24]

Limitations

We were not able to determine the rate of progression of aortic dilatation and stiffness because this study was cross-sectional. Another limitation was the relatively small number of control participants. In some patients, assessment of E_{inc} and PWV was not possible because of metal artifacts from surgical implants and early awakening from sedation. We further acknowledge the limitation of using noninvasive arterial blood pressures, rather than invasive blood pressures, for distensibility calculation for reasons of safety and ethics; however, all automated blood measurements were taken carefully at the time of the CMR study.

Because of the requirement to acquire cine magnetic resonance images without suspending the respiration of sedated patients, the spatial resolution was not sufficiently high to accurately detect structural aortic wall changes.

We did not perform a 3-dimensional analysis of aortic dilatation patterns and did not analyze aortic flow with 4-dimensional phase-contrast imaging. Future studies with 4-dimensional phase-contrast imaging are warranted to give more insight into the relationship between aortic size and blood flow patterns.

The E_{inc} of the aortic vessel wall was determined indirectly in this study through the Moens–Korteweg equation. Consequently, the estimation of E_{inc} is based on the premise that the Moens–Korteweg equation provides an accurate description of the relationship of PWV, E_{inc}, and vessel dimensions.

Three control participants were referred for CMR because of suspected aortic arch abnormality, but CMR findings were normal. This may raise concerns about the inclusion of these persons as healthy control participants. All comparisons between HLHS patients and healthy control participants were repeated with the 3 control participants who underwent CMR excluded. This did not materially alter the results of the study.

Conclusion

In HLHS patients, dilatation of the DAo is frequent and is associated with increased aortic arch E_{inc}, suggesting that the elastic properties of the aortic arch could lead to adverse vessel wall changes in the DAo. Because aortic dilatation and stiffness are well-known cardiovascular risk factors, this study should increase clinical awareness of potential complications of the DAo in HLHS patients. In addition, the observed changes further increase the afterload of systemic circulation and likely contribute to the burden of the systemic right ventricle, requiring thorough monitoring for early onset of right ventricular failure. Future studies using 4-dimensional phase-contrast imaging may give more insight into aortic blood flow patterns and their contribution to aortic pathologies in children with surgically palliated HLHS.

Acknowledgments

The authors thank Traudel Hansen, (CMR technologist) for her valuable assistance with patient management, and monitoring and follow-up during and after CMR.

Disclosures

None.

References

1. Voges I, Jerosch-Herold M, Hedderich J, Westphal C, Hart C, Helle M, Scheewe J, Pardun E, Kramer HH, Rickers C. Maladaptive aortic properties in children after palliation of hypoplastic left heart syndrome by cardiovascular magnetic resonance imaging. *Circulation*. 2010;122:1068–1076.
2. Biglino G1, Schievano S, Steeden JA, Ntsinjana H, Baker C, Khambadkone S, de Leval MR, Hsia TY, Taylor AM, Giardini A; Modeling of Congenital Hearts Alliance (MOCHA) Collaborative Group. Reduced ascending aorta distensibility relates to adverse ventricular mechanics in patients with hypoplastic left heart syndrome: noninvasive study using wave intensity analysis. *J Thorac Cardiovasc Surg*. 2012;144:1307–1313.
3. Cardis BM, Fyfe DA, Mahle WT. Elastic properties of the reconstructed aorta in hypoplastic left heart syndrome. *Ann Thorac Surg*. 2006;81:988–991.
4. Voges I, Jerosch-Herold M, Hedderich J, Pardun E, Hart C, Gabbert DD, Hansen JH, Petko C, Kramer HH, Rickers C. Normal values of aortic dimensions, distensibility, and pulse wave velocity in children and young adults: a cross-sectional study. *J Cardiovasc Magn Reson*. 2012;14:77.

5. Nollen GJ, Groenink M, Tijssen JG, Van Der Wall EE, Mulder BJ. Aortic stiffness and diameter predict progressive aortic dilatation in patients with Marfan syndrome. *Eur Heart J*. 2004;25:1146–1152.
6. Fielden SW, Fornwalt BK, Jerosch-Herold M, Eisner RL, Stillman AE, Oshinski JN. A new method for the determination of aortic pulse wave velocity using cross-correlation on 2D PCMR velocity data. *J Magn Reson Imaging*. 2008;27:1382–1387.
7. Gosling RG, Budge MM. Terminology for describing the elastic behaviors of arteries. *Hypertension*. 2003;41:1180–1182.
8. Groenink M, de Roos A, Mulder BJ, Verbeeten B Jr, Timmermans J, Zwinderman AH, Spaan JA, van der Wall EE. Biophysical properties of the normal-sized aorta in patients with Marfan syndrome: evaluation with MR flow mapping. *Radiology*. 2001;219:535–540.
9. Arndt JO, Stegall HF, Wicke HJ. Mechanics of the aorta in vivo. A radiographic approach. *Circ Res*. 1971;28:693–704.
10. den Reijer PM, Sallee D III, van der Velden P, Zaaijer ER, Parks WJ, Ramamurthy S, Robbie TQ, Donati G, Lamphier C, Beekman RP, Brummer ME. Hemodynamic predictors of aortic dilatation in bicuspid aortic valve by velocity-encoded cardiovascular magnetic resonance. *J Cardiovasc Magn Reson*. 2010;12:4.
11. Bissell MM, Hess AT, Biasiolli L, Glaze SJ, Loudon M, Pitcher A, Davis A, Prendergast B, Markl M, Barker AJ, Neubauer S, Myerson SG. Aortic dilation in bicuspid aortic valve disease: flow pattern is a major contributor and differs with valve fusion type. *Circ Cardiovasc Imaging*. 2013;6:499–507.
12. Chiu JJ, Chien S. Effects of disturbed flow on vascular endothelium: pathophysiological basis and clinical perspectives. *Physiol Rev*. 2011;91:327–387.
13. de Sa M, Moshkovitz Y, Butany J, David TE. Histologic abnormalities of the ascending aorta and pulmonary trunk in patients with bicuspid aortic valve disease: clinical relevance to the Ross procedure. *J Thorac Cardiovasc Surg*. 1999;118:588–596.
14. Roach Margo R. 1979. Hemodynamic factors in arterial stenosis and poststenotic dilatation. In: Stehbens WE, ed. *Hemodynamics and the Blood Vessel Wall*. III. Springfield: Charles C Thomas; 439–464.
15. Niwa K, Perloff JK, Bhuta SM, Laks H, Drinkwater DC, Child JS, Miner PD. Structural abnormalities of great arterial walls in congenital heart disease: light and electron microscopic analyses. *Circulation*. 2001;103:393–400.
16. Cavalcante JL, Lima JA, Redheuil A, Al-Mallah MH. Aortic stiffness: current understanding and future directions. *J Am Coll Cardiol*. 2011;57:1511–1522.
17. Boutouyrie P, Fliser D, Goldsmith D, Covic A, Wiecek A, Ortiz A, Martinez-Castelao A, Lindholm B, Massy ZA, Suleymanlar G, Sicari R, Gargani L, Parati G, Mallamaci F, Zoccali C, London GM. Assessment of arterial stiffness for clinical and epidemiological studies: methodological considerations for validation and entry into the European Renal and Cardiovascular Medicine registry. *Nephrol Dial Transplant*. 2014;29:232–239.
18. Payne RA, Webb DJ. Arterial blood pressure and stiffness in hypertension: is arterial structure important? *Hypertension*. 2006;48:366–367.
19. Van Bortel LM, Laurent S, Boutouyrie P, Chowienczyk P, Cruickshank JK, De Backer T, Filipovsky J, Huybrechts S, Mattace-Raso FU, Protogerou AD, Schillaci G, Segers P, Vermeersch S, Weber T; on behalf of the Artery Society, the European Society of Hypertension Working Group on Vascular Structure and Function and the European Network for Noninvasive Investigation of Large Arteries. Expert consensus document on the measurement of aortic stiffness in daily practice using carotid-femoral pulse wave velocity. *J Hypertens*. 2012;30:445–454.
20. Weigang E, Kari FA, Beyersdorf F, Luehr M, Etz CD, Frydrychowicz A, Harloff A, Markl M. Flow-sensitive four-dimensional magnetic resonance imaging: flow patterns in ascending aortic aneurysms. *Eur J Cardiothorac Surg*. 2008;34:11–16.
21. Sehested J, Baandrup U, Mikkelsen E. Different reactivity and structure of the prestenotic and poststenotic aorta in human coarctation. Implications for baroreceptor function. *Circulation*. 1982;65:1060–1065.
22. Laurent S, Kingwell B, Bank A, Weber M, Struijker-Boudier H. Clinical applications of arterial stiffness: therapeutics and pharmacology. *Am J Hypertens*. 2002;15:453–458.
23. Sundareswaran KS, Kanter KR, Kitajima HD, Krishnankutty R, Sabatier JF, Parks WJ, Sharma S, Yoganathan AP, Fogel M. Impaired power output and cardiac index with hypoplastic left heart syndrome: a magnetic resonance imaging study. *Ann Thorac Surg*. 2006;82:1267–1275.
24. Najjar SS, Scuteri A, Shetty V, Wright JG, Muller DC, Fleg JL, Spurgeon HP, Ferrucci L, Lakatta EG. Pulse wave velocity is an independent predictor of the longitudinal increase in systolic blood pressure and of incident hypertension in the Baltimore Longitudinal Study of Aging. *J Am Coll Cardiol*. 2008;51:1377–1383.